

The Carleman-Newton method to globally reconstruct a source term for nonlinear parabolic equation

Anuj Abhishek*[†] Thuy T. Le* Loc H. Nguyen* Taufiqar Khan*

Abstract

We propose to combine the Carleman estimate and the Newton method to solve an inverse source problem for nonlinear parabolic equations from lateral boundary data. The stability of this inverse source problem is conditionally logarithmic. Hence, numerical results due to the conventional least squares optimization might not be reliable. In order to enhance the stability, we approximate this problem by truncating the high frequency terms of the Fourier series that represents the solution to the governing equation. By this, we derive a system of nonlinear elliptic PDEs whose solution consists of Fourier coefficients of the solution to the parabolic governing equation. We solve this system by the Carleman-Newton method. The Carleman-Newton method is a newly developed algorithm to solve nonlinear PDEs. The strength of the Carleman-Newton method includes (1) no good initial guess is required and (2) the computational cost is not expensive. These features are rigorously proved. Having the solutions to this system in hand, we can directly compute the solution to the proposed inverse problem. Some numerical examples are displayed.

Key words: numerical methods; Carleman estimate; Carleman-Newton; boundary value problems; quasilinear elliptic equations; source term

AMS subject classification: 35R30, 35K55

1 Introduction

This paper belongs to a series of works to solve inverse problems for nonlinear partial differential equations [23, 31, 34]. In particular, we aim to globally solve an inverse source problem for nonlinear parabolic equations. By “globally”, we mean that our algorithm does not require *a priori* knowledge of the true solution. This feature is a significant strength of our method in comparison to the widely-used methods based on least square optimizations, which are locally convergent. Let $d \geq 2$ be the spatial dimension. Let $F : \mathbb{R}^d \times \mathbb{R} \times \mathbb{R}^d \rightarrow \mathbb{R}$ be a function in the class $C^1(\bar{\Omega})$ and T be a positive number. Consider the following initial value problem of nonlinear parabolic equation

$$\begin{cases} u_t = \Delta u + F(\mathbf{x}, u, \nabla u) & (\mathbf{x}, t) \in \mathbb{R}^d \times (0, T), \\ u(\mathbf{x}, 0) = p(\mathbf{x}) & \mathbf{x} \in \mathbb{R}^d. \end{cases} \quad (1.1)$$

Here, p is a source term. Let Ω be an open and bounded domain of \mathbb{R}^d . Assume that Ω has a smooth boundary $\partial\Omega$. Denote by Ω_T and $\partial\Omega_T$ the set $\Omega \times (0, T)$ and $\partial\Omega \times (0, T)$ respectively.

*Department of Mathematics and Statistics, University of North Carolina at Charlotte, Charlotte, NC, 28223, USA.

[†]Corresponding author, email: anuj.abhishek@uncc.edu.

We are interested in the problem of computing the source term p from the measurement of lateral information of the function u . More precisely, we solve the following problem.

Problem 1.1 (Inverse source problem). *Given the lateral data*

$$g_0(\mathbf{x}, t) = u(\mathbf{x}, t) \quad \text{and} \quad g_1(\mathbf{x}, t) = \partial_\nu u(\mathbf{x}, t) \quad (1.2)$$

for all $(\mathbf{x}, t) \in \partial\Omega_T$, determine the source term $p(\mathbf{x})$ for $\mathbf{x} \in \Omega$.

We only solve Problem 1.1 under the condition that (1.1) is uniquely solvable and its solution is bounded in C^1 .

More precisely, we impose the following condition on solution to (1.1).

Assumption 1.1. *Assume the source function p and the nonlinearity F are such that*

$$|u(\mathbf{x}, t)| + |\nabla u(\mathbf{x}, t)| \leq M \quad (1.3)$$

for a.e. $(\mathbf{x}, t) \in \Omega_T$ and for some number M depending only on p and F .

In general, due to the presence of the nonlinearity F , the well-posedness and regularity results for (1.1) are not guaranteed. In other words, Assumption 1.1 might not hold true. Some special conditions on F and p should be imposed. For completeness, we provide here a set of conditions that guarantees that (1.1) has a unique and bounded solution. Assume that $p(\mathbf{x})$ is in $H^{2+\alpha}(\mathbb{R}^d)$ for some $\alpha \in [0, 1 + 4/d]$. Assume further for all $\mathbf{x} \in \mathbb{R}^d$, $t \in [0, T]$, $s \in \mathbb{R}$, and $\xi \in \mathbb{R}^d$,

$$|F(\mathbf{x}, s, \xi)| \leq C \max \{ (1 + |\xi|)^2, 1 + |s| \} \quad (1.4)$$

for some positive constant C . Then, due to Theorem 6.1 in [19, Chapter 5, §6] and Theorem 2.1 in [19, Chapter 5, §2], problem (1.1) has a unique solution with a bounded C^1 norm.

Definition 1.1. *Fix a nonlinearity F . Denote by \mathcal{P} the set of all source functions $p \in H^1(\Omega)$ such that Assumption 1.1 holds true.*

In practice, the solution $p(\mathbf{x})$, $\mathbf{x} \in \Omega$, to Problem 1.1 might represent the initial distribution of the temperature or the initial stage of the pollutant. Therefore, computing p is important in many real-world applications, e.g., determination of the spatially distributed temperature inside a solid from the boundary measurement of the heat and heat flux in the time domain [15]; determining the level of pollutant on the surface of the rivers or lakes [7]; effective monitoring the heat conduction processes in steel industries, glass and polymer-forming and nuclear power station [28]. In the special case when the nonlinear term F takes the form $u(1 - u)$ (or $q(u) = u(1 - |u|^\alpha)$) for some $\alpha > 0$, the parabolic equation in (1.1) is called the high dimensional version of the well-known Fisher (or Fisher-Kolmogorov) equation [8]. Although the nonlinearity q does not satisfy condition (1.4), we do not experience any difficulty in numerical computations of the forward problem. It is worth mentioning that the Fisher equation occurs in ecology, physiology, combustion, crystallization, plasma physics, and in general phase transition problems, see [8]. Due to its realistic applications, the problem of determining the initial conditions of parabolic equations has been studied intensively. The uniqueness of Problem 1.1 for linear model was proved in [21]. The logarithmic stability results were rigorously proved in [15, 28]. Due to the presence of the nonlinear term $F(\mathbf{x}, u, \nabla u)$ in (1.1), the uniqueness and stability of Problem 1.1 might need to be proved, especially when the nonlinearity F might growth faster than the nonlinearity in [15, 28]. This task can be done by

combining Theorem 1 in [15] and a truncation technique. Since the proof is not complicated, we present this result here in this paper for the convenience of the reader.

Regarding constructive method, the widely used methods to solve inverse source problem like Problem 1.1 are based on optimization. In such methods, one typically optimizes a cost functional based on the problem. A prototypical example of a cost functional is

$$J(p) = \int_0^T \int_{\partial\Omega} [|L(p)(\mathbf{x}, t) - g_0(\mathbf{x}, t)|^2 + |\partial_\nu L(p)(\mathbf{x}, t) - g_1(\mathbf{x}, t)|^2] d\sigma(\mathbf{x}) dt + \text{a regularization term}$$

where $L(p) = u$ is the solution to (1.1). The minimizer of the cost functional serves as the computed solution to the inverse problem. Using this technique is challenging because inverse source problem for parabolic equation is severely ill-posed. The known stability is conditionally logarithmic (see [15, Theorem 1] and [28]), which is weaker than logarithmic. As a result, the reliability of numerical solutions due to these approaches might not be guaranteed, especially, in the case when significant noise is involved in the measured data. Another challenge in solving Problem 1.1 is the presence of the nonlinear term $F(\mathbf{x}, u, \nabla u)$, making the cost functional nonconvex. The cost functional might have multiple local minima and ravines. Hence, in general, to solve Problem 1.1, a good initial guess of the true solution is necessary. On the other hand, the expensive computational cost is another drawback of the optimization-based methods. Our new numerical approach proposed in this paper relaxes all drawbacks above. It is applicable to the data containing up to 20% of (multiplicative) noise. We name it Carleman-Newton method because it is suggested by Carleman estimates and the well-know Newton method in solving nonlinear equations.

We draw the reader's attention to the Carleman contraction principle, see [2, 4, 23, 22] to solve related problems to Problem 1.1. Like the proposed Carleman-Newton method, the Carleman contraction principle is very powerful since it can quickly solve nonlinear inverse problems without requesting a good initial guess. The new point of our paper in comparison to the cited publications above is that we allow F to depend on ∇u and we study the case when data contains noise. The case when F depends on ∇u arises from the field of Hamilton-Jacobi equations of the form $u_t = \epsilon \Delta u + F(\mathbf{x}, u, \nabla u)$, $0 < \epsilon \ll 1$ where the term $\epsilon \Delta u$ serves as the viscosity term. Hamilton-Jacobi equations are important in many fields; e.g. game theory and light propagation. Therefore, this gradient dependent case is worth studying. Rather than using the Carleman contraction principle as in [2, 4, 23, 22], we develop the Carleman-Newton method to solve the inverse problem under consideration. The Carleman-Newton method in this paper is stronger than the one introduced in [26]. In fact, we can prove a Lipschitz stability result of our proposed method with respect to the H^2 norm while the convergence in the cited papers above, as well as [26], is with respect to the H^1 norm. Another new point of this paper is that in the current paper, we study the noise analysis, which was missing in [26].

As mentioned, the best stability result for Problem 1.1 is conditionally logarithmic. Therefore, solving it is extremely challenging. To overcome this difficulty, we propose to solve Problem 1.1 in the Fourier domain truncating all high frequency components. More precisely, we derive a system of elliptic PDEs whose solution consists of a finite number of the Fourier coefficients of the solution to the parabolic equation (1.1). The solution of this system directly yields the knowledge of the function $u(\mathbf{x}, t)$, from which the solution to our inverse problem follows. We numerically solve this nonlinear system by the Carleman-Newton method suggested in [26]. The initial solution can be computed by solving the system obtained by removing the nonlinear term. Then, we approximate the nonlinear system by its linearization. Solving this approximation system, we find an updated solution. Continuing this process, we get a fast convergent sequence reaching to the desired function.

The convergence of this iterative procedure is rigorously proved by using a new Carleman estimate. The fast convergence will be shown in both analytic and numerical senses.

Some papers closely related to the current one are [4, 23, 22, 29]. On the other hand, the coefficient inverse problem for parabolic equations is also very interesting and studied intensively. We draw the reader's attention to [3, 5, 6, 11, 32, 36, 39] for important numerical methods and good numerical results. Besides, the problem of recovering the initial conditions for the hyperbolic equation is very interesting since it arises in many real-world applications. For instance, the problems thermo- and photo-acoustic tomography play the key roles in biomedical imaging. We refer the reader to some important works in this field [9, 10, 30]. Applying the Fourier transform, one can reduce the problem of reconstructing the initial conditions for hyperbolic equations to some inverse source problems for the Helmholtz equation, see [27, 35, 37, 38, 40] for some recent results.

The paper is organized as follows. In Section 2, we prove the uniqueness and the conditionally logarithmic stability results for Problem 1.1. In Section 3, we introduce an approximation context of Problem 1.1. In Section 4, we recall the Carleman-Newton method in [26]. In Section 5, we prove our main theorem about the convergence of the Carleman-Newton method. In Section 6, we present some numerical examples. Section 7 is for concluding remarks.

2 The uniqueness of the inverse source problem

In this section, we study the unique determination of the source function p from the given data. We have the following theorem.

Theorem 2.1. *Let p_1 and p_2 be in the set \mathcal{P} . Let u_1 and u_2 be solutions to (1.1) with p being replaced by p_1 and p_2 respectively. Let M_1 and M_2 be the numbers in the right hand side of (1.3) that correspond to p_1 and p_2 respectively. Let $B = \max\{M_1, M_2\}$. Then, there exists a constant C such that for all $\beta \in (0, 2)$, we can find a number $\epsilon_0 > 0$ such that*

$$\|p_1 - p_2\|_{L^2(\Omega)} \leq \frac{C}{\beta \ln[\frac{B}{\epsilon_0 e}]} \|\nabla(p_1 - p_2)\|_{L^2(\Omega)} + C \left(\frac{B}{\epsilon_0}\right)^\beta e^{2-\beta} \quad (2.1)$$

where

$$\mathbf{e} = \|u_1 - u_2\|_{H^1(\partial\Omega_T)} + \|\partial_\nu(u_1 - u_2)\|_{L^2(\partial\Omega_T)}. \quad (2.2)$$

represents the difference of two data corresponding to two source functions p_1 and p_2 .

Corollary 2.1 (The uniqueness of Problem 1.1). *It follows from (2.1) that by letting \mathbf{e} tend to 0, we obtain $p_1 = p_2$, which is basically the uniqueness of Problem 1.1.*

Proof of Theorem 2.1. Let $\chi_B : \bar{\Omega} \times \mathbb{R} \times \mathbb{R}^d \rightarrow [0, 1]$ be a cut off function in the class C^∞ that satisfies

$$\chi_B(\mathbf{x}, s, \mathbf{p}) = \begin{cases} 1 & 0 \leq |s| + |\mathbf{p}| \leq B \\ 0 & |s| + |\mathbf{p}| > 2B. \end{cases} \quad (2.3)$$

Define

$$F_B(\mathbf{x}, s, \mathbf{p}) = \chi_B(\mathbf{x}, s, \mathbf{p})F(\mathbf{x}, s, \mathbf{p}), \quad \text{for all } (\mathbf{x}, s, \mathbf{p}) \in \bar{\Omega} \times \mathbb{R} \times \mathbb{R}^d. \quad (2.4)$$

Since Assumption 1.1 holds true for p_1 and p_2 , we have

$$|u_i(\mathbf{x}, t)| + |\nabla u_i(\mathbf{x}, t)| \leq M_i \leq B$$

for $(\mathbf{x}, t) \in \overline{\Omega_T}$, $i \in \{1, 2\}$. Hence, both u_1 and u_2 satisfy the ‘‘cut off’’ parabolic equation

$$u_t = \Delta u + F_B(\mathbf{x}, u, \nabla u) \quad \text{for all } (\mathbf{x}, t) \in \overline{\Omega_T}. \quad (2.5)$$

Since F_B is smooth and has compact support, it is Lipschitz. There exists a constant $C_{F,B}$ depending only on F and B such that

$$|F_B(\mathbf{x}, s_1, \mathbf{p}_1) - F_B(\mathbf{x}, s_2, \mathbf{p}_2)| \leq C_{F,B}(|s_1 - s_2| + |\mathbf{p}_1 - \mathbf{p}_2|) \quad (2.6)$$

for all $\mathbf{x} \in \overline{\Omega}$, $s_1, s_2 \in \mathbb{R}$ and $\mathbf{p}_1, \mathbf{p}_2 \in \mathbb{R}^d$. Define $h = u_1 - u_2$. Due to (2.5) and (2.6),

$$\begin{aligned} |h_t(\mathbf{x}, t) - \Delta h(\mathbf{x}, t)| &= |F_B(\mathbf{x}, u_1(\mathbf{x}, t), \nabla u_1(\mathbf{x}, t)) - F_B(\mathbf{x}, u_2(\mathbf{x}, t), \nabla u_2(\mathbf{x}, t))| \\ &\leq C_{F,B}(|h(\mathbf{x}, t)| + |\nabla h(\mathbf{x}, t)|) \end{aligned} \quad (2.7)$$

for all $(\mathbf{x}, t) \in \overline{\Omega_T}$. It is obvious that

$$\mathbf{e} = \|h\|_{H^1(\partial\Omega_T)} + \|\partial_\nu h\|_{L^2(\partial\Omega_T)}.$$

Fix $\beta \in (0, 2)$. Using (2.7) and applying Theorem 1 in [15] for the function h , we can find a constant $C > 0$ and a number $\epsilon_0 \in (0, 1)$ such that

$$\|h(\mathbf{x}, 0)\|_{L^2(\Omega)} \leq \frac{C}{\beta \ln[\frac{B}{\epsilon_0 e}]} \|\nabla h(\mathbf{x}, 0)\|_{L^2(\Omega)} + C \left(\frac{B}{\epsilon_0}\right)^\beta e^{2-\beta}. \quad (2.8)$$

Estimate (2.1) is a direct consequence of (2.8). \square

Remark 2.1. *Although estimate (2.1) guarantees the uniqueness of Problem 1.1 (see Corollary 2.1), it does not lead to a reliable numerical approach to solve Problem 1.1. In fact, due to the presence of the term $\|\nabla(p_1 - p_2)\|_{L^2(\Omega)}$ in the right hand side of (2.1), we cannot obtain a stability result for Problem 1.1. Therefore, methods to solve Problem 1.1 based on optimization might not provide reliable solutions.*

By Remark 2.1, rather than employing the optimization approach, to numerically solve Problem 1.1, we propose to regularize and approximate the inverse problem by truncating the high frequency components of the solution to (1.1). This idea was introduced in [16]. Then, it was successfully used in many projects of our research group; see e.g. [14, 23, 24]. Details will be given in the next section.

3 A numerical method to solve Problem 1.1

Our method to stably solve Problem 1.1 consists of two stages. In stage 1, we derive a ‘‘Garlekin-Fourier’’ approximation model of (1.1). In stage 2, we solve that approximation model by the Carleman-Newton method, first introduced in [26]. Stage 1 is presented in this section while we will develop a numerical method for Stage 2 in Sections 4 and 5.

Motivated by [23] and Remark 2.1, we solve Problem 1.1 by establishing a system of quasi-linear partial differential equations with Cauchy boundary data. This system will be solved later by the method proposed in [26]. Let $\{\Psi_n\}_{n \geq 1}$ be an orthonormal basis of $L^2(0, T)$. We approximate the solution u to (1.1) by truncating its Fourier expansion with respect to the basis $\{\Psi_n\}_{n \geq 1}$ as follows

$$u(\mathbf{x}, t) = \sum_{n=1}^{\infty} u_n(\mathbf{x}) \Psi_n(t) \simeq \sum_{n=1}^N u_n(\mathbf{x}) \Psi_n(t) \quad (3.1)$$

for $(\mathbf{x}, t) \in \overline{\Omega_T}$ where

$$u_n(\mathbf{x}) = \int_0^T u(\mathbf{x}, t) \Psi_n(t) dt \quad (3.2)$$

for some “cut off” number N . The cut off number N will be numerically chosen later. We also approximate $u_t(\mathbf{x}, t)$, $(\mathbf{x}, t) \in \overline{\Omega_T}$, by

$$u_t(\mathbf{x}, t) \simeq \sum_{n=1}^N u_n(\mathbf{x}) \Psi'_n(t). \quad (3.3)$$

From now on, we assume that the approximations in (3.1) and (3.3) are valid in the sense that the resulting errors are sufficiently small. This assumption is acceptable in computation. It is somewhat similar to the main principle in Galerkin approximation, in which we approximate the function $u(\mathbf{x}, \cdot)$ by using a finite number of elements in the orthonormal basis $\{\Psi_n\}_{n \geq 1}$ of $L^2(0, T)$. Plugging (3.1) and (3.3) into (1.1), we obtain

$$\sum_{n=1}^N u_n(\mathbf{x}) \Psi'_n(t) = \sum_{n=1}^N \Delta u_n(\mathbf{x}) \Psi_n(t) + F\left(\mathbf{x}, \sum_{n=1}^N u_n(\mathbf{x}) \Psi_n(t), \sum_{n=1}^N \nabla u_n(\mathbf{x}) \Psi_n(t)\right) \quad (3.4)$$

for all $(\mathbf{x}, t) \in \overline{\Omega_T}$. For each $m \in \{1, \dots, N\}$, we multiply the function Ψ_m to both sides of (3.4) and integrate the resulting equation with respect to t . We obtain

$$\begin{aligned} \sum_{n=1}^N u_n(\mathbf{x}) \int_0^T \Psi'_n(t) \Psi_m(t) dt &= \sum_{n=1}^N \Delta u_n(\mathbf{x}) \int_0^T \Psi_n(t) \Psi_m(t) dt \\ &\quad + \int_0^T F\left(\mathbf{x}, \sum_{n=1}^N u_n(\mathbf{x}) \Psi_n(t), \sum_{n=1}^N \nabla u_n(\mathbf{x}) \Psi_n(t)\right) \Psi_m(t) dt \end{aligned} \quad (3.5)$$

for all $\mathbf{x} \in \overline{\Omega}$. For $m, n \in \{1, \dots, N\}$ and $\mathbf{x} \in \overline{\Omega}$, define

$$s_{mn} = \int_0^T \Psi'_n(t) \Psi_m(t) dt, \quad (3.6)$$

$$\mathfrak{f}_m(\mathbf{x}, U, \nabla U) = \int_0^T F\left(\mathbf{x}, \sum_{n=1}^N u_n(\mathbf{x}) \Psi_n(t), \sum_{n=1}^N \nabla u_n(\mathbf{x}) \Psi_n(t)\right) \Psi_m(t) dt \quad (3.7)$$

where $U = (u_1, u_2, \dots, u_N)^T$. Denote by S and $\mathcal{F}(\mathbf{x}, U, \nabla U)$ the matrix $(s_{mn})_{m,n=1}^N$ and the vector $(\mathfrak{f}_m(\mathbf{x}, U, \nabla U))_{m=1}^N$ respectively. Since

$$\int_0^T \Psi_n(t) \Psi_m(t) dt = \begin{cases} 1 & m = n, \\ 0 & m \neq n, \end{cases}$$

it follows from (3.5) that

$$\Delta U - SU + \mathcal{F}(\mathbf{x}, U, \nabla U) = 0 \quad \text{for all } \mathbf{x} \in \Omega. \quad (3.8)$$

On the other hand, due to (1.2) and (3.2), we have for all $m \in \{1, \dots, N\}$ and $\mathbf{x} \in \partial\Omega$,

$$u_m(\mathbf{x}) = \int_0^T g_0(\mathbf{x}, t) \Psi_m(t) dt, \quad (3.9)$$

$$\partial u_m(\mathbf{x}) = \int_0^T g_1(\mathbf{x}, t) \Psi_m(t) dt. \quad (3.10)$$

For $\mathbf{x} \in \partial\Omega$, define

$$G_0(\mathbf{x}) = \left(\int_0^T g_0(\mathbf{x}, t) \Psi_m(t) dt \right)_{m=1}^N, \quad (3.11)$$

$$G_1(\mathbf{x}) = \left(\int_0^T g_1(\mathbf{x}, t) \Psi_m(t) dt \right)_{m=1}^N. \quad (3.12)$$

It follows from (3.8)–(3.12), the vector U satisfies the Cauchy like boundary problem

$$\begin{cases} \Delta U - SU + \mathcal{F}(\mathbf{x}, U, \nabla U) = 0 & \mathbf{x} \in \Omega, \\ U(\mathbf{x}) = G_0(\mathbf{x}) & \mathbf{x} \in \partial\Omega, \\ \partial_\nu U(\mathbf{x}) = G_1(\mathbf{x}) & \mathbf{x} \in \partial\Omega. \end{cases} \quad (3.13)$$

In the next section, we combine a Carleman estimate and the Newton method to compute a solution U to (3.13). Once this step is done, Problem 1.1 is solved. In fact, having U in hand, we can compute $u(\mathbf{x}, t)$ via (3.1). The desired function $p(\mathbf{x})$ is given by $u(\mathbf{x}, 0)$ for all $\mathbf{x} \in \Omega$.

Remark 3.1. *Due to the cut off in (3.1), system (3.13) is not exact. We called it an approximation model. As mentioned in Remark 2.1, directly solving the inverse problem with the optimization method may be problematic since the stability is just conditionally logarithmic. In contrast, by a step of approximation, we derive a system of elliptic equations with Cauchy data. It is well-known that solving elliptic equations with full boundary conditions is stable. This promises the success for our numerical study. This cut off technique was used to solve several different types of inverse problems; see e.g. [12, 13, 14, 23, 25, 32, 36, 31]. In contrast, proving the convergence of (3.13) as $N \rightarrow \infty$ is extremely challenging. Studying the behavior of (3.13) as $N \rightarrow \infty$ is out of the scope of the paper.*

4 The Carleman-Newton method

Currently, there are at least three different Carleman based methods to solve (3.13):

1. *The convexification method.* The main idea of the convexification method to solve (3.13) is to minimize the Carleman weighted functional

$$U \mapsto \int_{\Omega} W_\lambda(\mathbf{x}) |\Delta U - SU + \mathcal{F}(\mathbf{x}, U, \nabla U)|^2 d\mathbf{x} + \text{a regularization term} \quad (4.1)$$

subject to the given boundary conditions for some Carleman weight function $W_\lambda(\mathbf{x})$. With suitable choice of $W_\lambda(\mathbf{x})$ and the regularization term, one can prove that the functional in (4.1) is strictly convex in any bounded set of $H^s(\Omega)^N$ where $s > [d/2] + 2$. The strict convexity implies that the minimizer is unique. Two other important theoretical results for the convexification method are (1) the minimizer can be obtained by using the conventional gradient descent method and the (2) the minimizer is an approximation of the desired solution to (3.13). The original idea about the convexification method is introduced in [17]. See [1, 14, 24, 18] for follow-up results. Although effective in delivering good numerical solutions, the convexification method has a drawback. It is time consuming. We therefore do not employ the convexification method in this paper.

2. *The Carleman contraction method.* The main idea of the contraction method to solve (3.13) is that we take an arbitrary function $U_0 \in H^2(\Omega)^N$. Assume that U_n is known, we compute U_{n+1} by solving

$$\begin{cases} \Delta U_{n+1} - S U_{n+1} + \mathcal{F}(\mathbf{x}, U_n, \nabla U_n) = 0 & \mathbf{x} \in \Omega, \\ U_{n+1}(\mathbf{x}) = G_0(\mathbf{x}) & \mathbf{x} \in \partial\Omega, \\ \partial_\nu U_{n+1}(\mathbf{x}) = G_1(\mathbf{x}) & \mathbf{x} \in \partial\Omega. \end{cases} \quad (4.2)$$

by using the quasi-reversibility method [20] combining with a suitable Carleman weight function as in [23]. One can follow the arguments in [23, 33] to prove the convergence of the constructed sequence $\{U_n\}_{n \geq 0}$ to the true solution to (3.13). For more details, see the following papers [22, 23, 33, 31]. This method was used to solve a similar inverse problem to Problem 1.1. We therefore do not repeat it in this paper.

3. The Carleman method combining with linearization [26]. We name this method Carleman-Newton method. Details of this method will be given in this section.

All three methods above are effective in solving quasi-linear PDEs. In this paper, we use method 3. We choose method 3 because it is quite powerful in the sense that we have already successfully applied it to compute viscosity solutions to a large class of Hamilton-Jacobi equations in [26].

4.1 A heuristic approach based on the Newton method

To express the idea behind numerical method 3, we recall here the well-known Newton method to solve nonlinear algebraic equation $f(x) = 0$ for $x \in \mathbb{R}$. In applying this method, one begins by choosing an initial guess for the solution, say x_0 . Let l_0 be the tangent line to the graph of the function f at x_0 . One finds the intersection of l_0 to the x -axis, called x_1 . Let l_1 be the tangent line to the graph of the function f at x_1 . One finds the intersection of l_1 to the x -axis, called x_2 . Continuing this procedure, one can obtain a sequence $\{x_n\}_{n \geq 0}$. Under the usual convexity assumptions on f , this sequence converges to the solution to the equation $f(x) = 0$. We combine the idea of the Newton method and a Carleman estimate to solve nonlinear PDEs of the form (3.13). It is important to mention that this combination is fairly powerful in the sense that the convergence of the constructed sequence to the true solution to (3.13) is guaranteed regardless of the distance from initial guess to the true solution.

We solve (3.13) in the strong sense. That means we compute a vector valued function U in $H^2(\Omega)^N$ that is the “best fit” (3.13). In the analysis, we will use the notation

$$H = \{V \in H^2(\Omega)^N : V|_{\partial\Omega} = G_0 \text{ and } \partial_\nu V|_{\partial\Omega} = G_1\}. \quad (4.3)$$

and

$$H_0 = \{V \in H^2(\Omega)^N : V|_{\partial\Omega} = 0 \text{ and } \partial_\nu V|_{\partial\Omega} = 0\}. \quad (4.4)$$

The set H is called the set of admissible solutions and the set H_0 is clearly a closed subspace of $H^2(\Omega)^N$. Define the operator

$$\mathcal{L}(U) = \Delta U - S U + \mathcal{F}(\mathbf{x}, U, \nabla U) \quad (4.5)$$

for all vector valued function $U \in H$. Heuristically, we want to solve the equation $\mathcal{L}U = 0$ in H . Let U_0 be an arbitrary initial function $U_0 \in H$. Based on the Newton method, we set $U_1 = U_0 + h_1 \in H$

where h_1 solves

$$\begin{cases} \mathcal{L}(U_0) + \Delta h_1 - S h_1 + D\mathcal{F}(\mathbf{x}, U_0, \nabla U_0)(h_1) = 0 & \mathbf{x} \in \Omega, \\ h_1 = 0 & \mathbf{x} \in \partial\Omega, \\ \partial_\nu h_1 = 0 & \mathbf{x} \in \partial\Omega. \end{cases} \quad (4.6)$$

In (4.6),

$$D\mathcal{F}(x, \mathbf{b}, A)(h_1) = \left(\nabla_{\mathbf{b}} f_m(\mathbf{x}, \mathbf{b}, A) \cdot h_1 + \nabla_A f_m(\mathbf{x}, \mathbf{b}, A) : \nabla h_1 \right)_{m=1}^N \quad (4.7)$$

for all $\mathbf{b} \in \mathbb{R}^N$ and $A \in \mathbb{R}^{N \times d}$. In (4.7), the notations “ \cdot ” and “ $:$ ” are the usual inner products in \mathbb{R}^N and in $\mathbb{R}^{N \times d}$ respectively. Repeating the process replacing U_0 by U_1 , we can find $U_2 \in H$ and then a sequence $\{U_n\}_{n \geq 0} \in H$. More precisely, for each $n \geq 1$, we define $U_n = U_{n-1} + h_n$ where h_n solves

$$\begin{cases} \mathcal{L}(U_{n-1}) + \Delta h_n - S h_n + D\mathcal{F}(\mathbf{x}, U_{n-1}, \nabla U_{n-1})(h_n) = 0 & \mathbf{x} \in \Omega, \\ h_n = 0 & \mathbf{x} \in \partial\Omega, \\ \partial_\nu h_n = 0 & \mathbf{x} \in \partial\Omega. \end{cases} \quad (4.8)$$

Due to both Dirichlet and Neumann boundary conditions, both problems (4.6) and (4.8) are over-determined. They might not have a solution. However, this difficulty does not lead to any error in our analysis. The main reason is that we only need to find their “best fit” solutions by the Carleman quasi-reversibility method. See Section 4.2 for a brief discussion about the Carleman quasi-reversibility method.

Remark 4.1. *In general, since we do not impose any special structure for the nonlinearity F , the vector \mathcal{F} has no special structure, either. In this general case, there is no guarantee for the convergence of the sequence $\{U_n\}_{n \geq 0}$ to the true solution to (3.13), especially when U_0 is far away from the true solution to (3.13). However, we have figured out in [26] that when we employ the Carleman quasi-reversibility method to solve (4.8) to construct the sequence $\{U_n\}_{n \geq 0}$, the desired convergence is true. In Section 5, we improve convergence result in [26] in the sense that the new convergence is in the H^2 norm while the similar convergence in [26] is with respect to the H^1 norm. On the other hand, in this paper we study a noise analysis, which was not done in [26]. Since this method is based on a Carleman estimate and is inspired by the Newton method, we name our approach the Carleman-Newton method.*

4.2 A Carleman estimate and the Carleman quasi-reversibility method

We recall a Carleman estimate, which serves as an important tool to prove the convergence of the Carleman Newton method to solve problem 3.13. We have the following lemma.

Lemma 4.1 (Carleman estimate, see [23]). *Let \mathbf{x}_0 be a point in $\mathbb{R}^d \setminus \bar{\Omega}$ such that $r(\mathbf{x}) = |\mathbf{x} - \mathbf{x}_0| > 1$ for all $\mathbf{x} \in \Omega$. Let $b > \max_{\mathbf{x} \in \bar{\Omega}} r(\mathbf{x})$ be a fixed constant. There exist positive constants β_0 depending only on b , \mathbf{x}_0 , Ω and d such that for all function $v \in C^2(\bar{\Omega})$ satisfying*

$$v(\mathbf{x}) = \partial_\nu v(\mathbf{x}) = 0 \quad \text{for all } \mathbf{x} \in \partial\Omega,$$

the following estimate holds true

$$\begin{aligned} \int_{\Omega} e^{2\lambda b^{-\beta} r^{\beta}(\mathbf{x})} |\Delta v(\mathbf{x})|^2 d\mathbf{x} &\geq \frac{C}{\lambda \beta^{7/4} b^{-\beta}} \int_{\Omega} e^{2\lambda b^{-\beta} r^{\beta}(\mathbf{x})} r^{2\beta}(\mathbf{x}) |D^2 v(\mathbf{x})|^2 d\mathbf{x} \\ &\quad + C \lambda^3 \beta^4 b^{-3\beta} \int_{\Omega} r^{2\beta}(\mathbf{x}) e^{2\lambda b^{-\beta} r^{\beta}} |v(\mathbf{x})|^2 d\mathbf{x} \\ &\quad + C \lambda \beta^{1/2} b^{-\beta} \int_{\Omega} e^{2\lambda b^{-\beta} r^{\beta}(\mathbf{x})} |\nabla v(\mathbf{x})|^2 d\mathbf{x} \end{aligned} \quad (4.9)$$

for $\beta \geq \beta_0$ and $\lambda \geq \lambda_0$. Here, $D^2 v = (v_{x_i x_j})_{i,j=1}^d$ is the Hessian matrix of v , $\lambda_0 = \lambda_0(b, \Omega, d, \mathbf{x}_0) > 1$ is a positive number with $\lambda_0 b^{-\beta} \gg 1$ and $C = C(b, \Omega, d, \mathbf{x}_0) > 1$ is a constant. These numbers depend only on listed parameters.

Corollary 4.1. Recall β_0 and λ_0 as in Lemma 4.1. Fix $\beta = \beta_0$ and let the constant C depend on \mathbf{x}_0 , Ω , d and β . There exists a constant λ_0 depending only on \mathbf{x}_0 , Ω , d and β such that for all function $v \in H^2(\Omega)$ with

$$v(\mathbf{x}) = \partial_\nu v(\mathbf{x}) = 0 \quad \text{on } \partial\Omega,$$

we have

$$\begin{aligned} \int_{\Omega} e^{2\lambda b^{-\beta} r^{\beta}(\mathbf{x})} |\Delta v(\mathbf{x})|^2 d\mathbf{x} &\geq C \lambda^{-1} \int_{\Omega} e^{2\lambda b^{-\beta} r^{\beta}(\mathbf{x})} |D^2 v(\mathbf{x})|^2 d\mathbf{x} \\ &\quad + C \lambda^3 \int_{\Omega} e^{2\lambda b^{-\beta} r^{\beta}} |v(\mathbf{x})|^2 d\mathbf{x} + C \lambda \int_{\Omega} e^{2\lambda b^{-\beta} r^{\beta}(\mathbf{x})} |\nabla v(\mathbf{x})|^2 d\mathbf{x} \end{aligned} \quad (4.10)$$

for all $\lambda \geq \lambda_0$.

We will now explain the Carleman quasi-reversibility method to solve (4.8). Let β_0 and λ_0 be as in Corollary 4.1. Fix $\beta = \beta_0$. For $\lambda > \lambda_0$, given a vector valued function $U_{n-1} \in H$, $n \geq 1$, we say that

$$\begin{aligned} h_n = \operatorname{argmin}_{\varphi \in H_0} \left[\int_{\Omega} e^{2\lambda b^{-\beta} r^{\beta}(\mathbf{x})} |\Delta \varphi - S\varphi + D\mathcal{F}(\mathbf{x}, U_{n-1}, \nabla U_{n-1})(\varphi) + \mathcal{L}(U_{n-1})|^2 d\mathbf{x} \right. \\ \left. + \epsilon \|U_{n-1} + \varphi\|_{H^2(\Omega)^N}^2 \right] \end{aligned} \quad (4.11)$$

is the solution to (4.8) due to the Carleman quasi-reversibility method. The number $\epsilon \in (0, 1)$ is called the regularization parameter. The presence of the Carleman weight function $e^{2\lambda b^{-\beta} r^{\beta}(\mathbf{x})}$ is the key for us to establish the convergence result in this paper. The important role of this Carleman weight function suggests the name Carleman quasi-reversibility method. The quasi-reversibility method without the presence of a Carleman weight function was first introduced in [20]. The convergence of the quasi-reversibility method as $\epsilon \rightarrow 0$ was proved in [32].

Remark 4.2. The unique minimizer in (4.11) can be proved by using the same arguments in [22, Theorem 4.1]. For brevity, we do not repeat the proof here. By using the Carleman quasi-reversibility method, we do not find the exact solution to (4.8). Rather, we compute the best fit solution h_n . This feature is important because (4.8) might not have a solution. When (4.8) does have a solution, the reader can find the proof of the convergence of this best fit solution to the true solution as $\epsilon \rightarrow 0$ in [32].

Inspired by the heuristic arguments in Section 4.1, we propose Algorithm 1 to numerically solve (3.13). The main aim of this section is to prove the efficiency of this algorithm.

Algorithm 1 The procedure to compute the numerical solution to (3.13)

- 1: Choose a regularized parameter $0 < \epsilon \ll 1$, a Carleman weight function $e^{2\lambda b^{-\beta} r^\beta}$, and a threshold number $0 < \kappa_0 \ll 1$.
- 2: Choose an initial solution $U_0 \in H$.
- 3: Set $n = 1$.
- 4: Let $U_n = U_{n-1} + h_n$ where $h_n \in H_0$ is the minimizer of $J_{n-1} : H_0 \rightarrow \mathbb{R}$ defined as

$$J_{n-1}(\varphi) = \int_{\Omega} e^{2\lambda b^{-\beta} r^\beta(\mathbf{x})} |\Delta\varphi - S\varphi + D\mathcal{F}(\mathbf{x}, U_{n-1}, \nabla U_{n-1})(\varphi) + \mathcal{L}(U_{n-1})|^2 d\mathbf{x} + \epsilon \|U_{n-1} + \varphi\|_{H^2(\Omega)}^2$$

for all $\varphi \in H_0$.

- 5: **if** $\|U_n - U_{n-1}\|_{L^\infty} \leq \kappa_0$ **then**
 - 6: Reassign $n := n + 1$.
 - 7: Go back to step 4.
 - 8: **else**
 - 9: Set the computed solution $U^{\text{comp}} = U_n$.
 - 10: **end if**
-

5 The global convergence of the Carleman-Newton method

The following result is one of the main theorems of this paper. We first consider the case when \mathcal{F} has a finite C^2 norm. If $\|\mathcal{F}\|_{C^2} = \infty$, we can apply the truncating technique in the proof of Theorem 2.1 to reduce the problem to the former case, see Remark 5.4 for details.

In this section, we consider the case when the observed data of Problem 1.1 are noisy. As a result, the values of the boundary data of (3.13) are not exact. Denote by G_0^δ and G_1^δ the noisy data with the noise level δ . It is worth mentioning that equation (3.13) with G_0 and G_1 replaced by G_0^δ and G_1^δ , respectively, might not have a solution. Let G_0^* and G_1^* be the noiseless versions of G_0 and G_1 respectively. By noise level δ , we mean that

$$\inf \{ \mathcal{E} \in H^2(\Omega)^N : \mathcal{E}|_{\partial\Omega} = G_0^\delta - G_0^* \text{ and } \partial_\nu \mathcal{E}|_{\partial\Omega} = G_1^\delta - G_1^* \} \leq \delta. \quad (5.1)$$

Due to (5.1), there is an error vector value function \mathcal{E} satisfying

$$\begin{cases} \|\mathcal{E}\|_{H^2(\Omega)} < 2\delta, \\ \mathcal{E}|_{\partial\Omega} = G_0^\delta - G_0^*, \\ \partial_\nu \mathcal{E}|_{\partial\Omega} = G_1^\delta - G_1^*. \end{cases} \quad (5.2)$$

Remark 5.1. *The existence of the error function \mathcal{E} in (5.2) implies that the noise must be the restriction of a vector valued function in $H^2(\Omega)$ onto $\partial\Omega$. Hence, the noise must be in $H^{3/2}(\partial\Omega)$. This assumption might not be realistic since the noise in measurement might be not smooth. There are several techniques to smooth out the noise; for e.g., the Tikhonov method and the b-spline method. However, in this paper, we do not have to apply one of these techniques to obtain numerical results. The proposed method works with nonsmooth data. That means, the Carleman-Newton method is stronger than what we can rigorously prove.*

Given the noisy data, the set of admissible solutions H , defined in (4.3), becomes

$$H^\delta = \{ V \in H^2(\Omega)^N : V|_{\partial\Omega} = G_0^\delta \text{ and } \partial_\nu V|_{\partial\Omega} = G_1^\delta \}. \quad (5.3)$$

Since G_0^* and G_1^* contain no noise, we can assume that

$$\begin{cases} \Delta U^* - SU^* + \mathcal{F}(\mathbf{x}, U^*, \nabla U^*) = 0 & \mathbf{x} \in \Omega, \\ U^*(\mathbf{x}) = G_0^*(\mathbf{x}) & \mathbf{x} \in \partial\Omega, \\ \partial_\nu U^*(\mathbf{x}) = G_1^*(\mathbf{x}) & \mathbf{x} \in \partial\Omega \end{cases} \quad (5.4)$$

has a unique solution U^* .

Theorem 5.1. *Assume that the source function p is in the class \mathcal{P} and assume that $\|\mathcal{F}\|_{C^2} < \infty$. Let U_0 be a vector valued function in H^δ . Let $\{U_n\}_{n \geq 0}$ be the sequence constructed in Algorithm 1. Assume that (5.4) has a unique solution U^* . For $\lambda > \lambda_0$ and $\beta = \beta_0$ as in Corollary 4.1, we have*

$$\begin{aligned} & \int_{\Omega} e^{2\lambda b^{-\beta} r^\beta(\mathbf{x})} (\lambda^{-2} |D^2(U_n - U^*)|^2 + |U_n - U^*|^2 + |\nabla(U_n - U^*)|^2) d\mathbf{x} \\ & \leq \left(\frac{C}{\lambda}\right)^{n+1} \int_{\Omega} e^{\lambda b^{-\beta} r^\beta(\mathbf{x})} (\lambda^{-2} |D^2(U_0 - U^*)|^2 + |U_0 - U^*|^2 + |\nabla(U_0 - U^*)|^2) d\mathbf{x} \\ & \quad + \left(\frac{C}{\lambda}\right)^{n+1} \int_{\Omega} e^{\lambda b^{-\beta} r^\beta(\mathbf{x})} (\lambda^{-2} |D^2\mathcal{E}|^2 + |\mathcal{E}|^2 + |\nabla\mathcal{E}|^2) d\mathbf{x} \\ & \quad + \frac{C/\lambda}{1 - C/\lambda} \left[\int_{\Omega} e^{2\lambda b^{-\beta} r^\beta(\mathbf{x})} |\Delta\mathcal{E} - S\mathcal{E}|^2 d\mathbf{x} + \epsilon \|\mathcal{E}\|_{H^2(\Omega)^2}^2 + \epsilon \|U^*\|_{H^2(\Omega)^2}^2 \right] \end{aligned} \quad (5.5)$$

where C is a constant depending only on b , Ω , d and \mathbf{x}_0 .

Corollary 5.1. *Fix $\lambda > \lambda_0$ such that $\theta = C/\lambda \in (0, 1)$. It follows from (5.5) that*

$$\|U_n - U^*\|_{H^2(\Omega)^N}^2 \leq \theta^{n+1} \|U_0 - U^*\|_{H^2(\Omega)^N}^2 + \frac{C\theta}{1 - \theta} (\delta^2 + \epsilon \|U^*\|_{H^2(\Omega)^N}^2). \quad (5.6)$$

Hence, the sequence $\{U_n\}_{n \geq 0}$ strongly converges to U^* in the H^2 norm regardless of the initial distance from U_0 to U^* . The error caused by the noise and the regularization technique is $O(\delta + \sqrt{\epsilon})$.

Corollary 5.2. *Let $U^{\text{comp}} = U_n$ where n is as in Step 9 of Algorithm 1. Write $U^{\text{comp}} = (u_1^{\text{comp}}, \dots, u_N^{\text{comp}})^T$ and $U^* = (u_1^*, \dots, u_N^*)^T$. Define*

$$p^{\text{comp}}(\mathbf{x}) = \sum_{m=1}^N u_m^{\text{comp}}(\mathbf{x}) \Psi_m(0) \quad \text{and} \quad p^*(\mathbf{x}) = \sum_{m=1}^N u_m^*(\mathbf{x}) \Psi_m(0) \quad (5.7)$$

for all $\mathbf{x} \in \Omega$. Due to (5.6), we have

$$\|p^{\text{comp}} - p^*\|_{H^2(\Omega)^N}^2 \leq C\theta^{n+1} \|U_0 - U^*\|_{H^2(\Omega)^N}^2 + \frac{C\theta}{1 - \theta} (\delta^2 + \epsilon \|U^*\|_{H^2(\Omega)^N}^2). \quad (5.8)$$

Estimate (5.8) guarantee the convergence of Algorithm 1.

Remark 5.2. *Due to (5.8), the convergence of the method is $O(\theta^n)$ as $n \rightarrow \infty$, which is exponentially fast. Hence, the computational cost is not expensive. On the other hand, the error in computation is $O(\delta + \sqrt{\epsilon})$ as $(\delta, \epsilon) \rightarrow (0, 0)$.*

Remark 5.3. *The proof of Theorem 5.1 is similar to that of [26, Theorem 4.1] with suitable modifications. These modifications are to improve the quality of the convergence. In fact, the new convergence is with respect to the H^2 norm while the convergence in [26, Theorem 4.1] is with respect to the H^1 norm. Moreover, no noise analysis was done in [26, Theorem 4.1] while the Lipschitz stability with respect to the noise is shown in (5.6).*

Proof of Theorem 5.1. Fix $n \geq 1$. Since h_n defined in Step 4 of Algorithm 1 is the minimizer of J_{n-1} in H_0 , by the variational principle, the Fréchet derivative $DJ_{n-1}(h_n)(\varphi)$ vanishes for all $\varphi \in H_0$. We have

$$\int_{\Omega} e^{2\lambda b^{-\beta} r^{\beta}(\mathbf{x})} [\Delta h_n - S h_n + D\mathcal{F}(\mathbf{x}, U_{n-1}, \nabla U_{n-1})(h_n) + \mathcal{L}(U_{n-1})] \cdot [\Delta \varphi - S \varphi + D\mathcal{F}(\mathbf{x}, U_{n-1}, \nabla U_{n-1})(\varphi)] d\mathbf{x} + \epsilon \langle U_{n-1} + h_n, \varphi \rangle_{H^2(\Omega)^N} = 0 \quad (5.9)$$

for all $\varphi \in H_0$. Due to the definition of U_n in Step 4 of Algorithm 1, we have $h_n = U_n - U_{n-1}$. This, together with the definition of the operator \mathcal{L} in (4.5) and the identity (5.9), gives

$$\int_{\Omega} e^{2\lambda b^{-\beta} r^{\beta}(\mathbf{x})} [\Delta U_n - S U_n + \mathcal{F}(\mathbf{x}, U_{n-1}, \nabla U_{n-1}) + D\mathcal{F}(\mathbf{x}, U_{n-1}, \nabla U_{n-1})(U_n - U_{n-1})] \cdot [\Delta \varphi - S \varphi + D\mathcal{F}(\mathbf{x}, U_{n-1}, \nabla U_{n-1})(\varphi)] d\mathbf{x} + \epsilon \langle U_n, \varphi \rangle_{H^2(\Omega)^N} = 0 \quad (5.10)$$

for all $\varphi \in H_0$. On the other hand, since U^* is a solution to (5.4), we have

$$\int_{\Omega} e^{2\lambda b^{-\beta} r^{\beta}(\mathbf{x})} [\Delta U^* - S U^* + \mathcal{F}(\mathbf{x}, U^*, \nabla U^*)] \cdot [\Delta \varphi - S \varphi + D\mathcal{F}(\mathbf{x}, U_{n-1}, \nabla U_{n-1})(\varphi)] d\mathbf{x} = 0 \quad (5.11)$$

for all $\varphi \in H_0$. Combining (5.10) and (5.11), we obtain

$$\int_{\Omega} e^{2\lambda b^{-\beta} r^{\beta}(\mathbf{x})} [\Delta(U_n - U^*) - S(U_n - U^*) + \mathcal{F}(\mathbf{x}, U_{n-1}, \nabla U_{n-1}) + D\mathcal{F}(\mathbf{x}, U_{n-1}, \nabla U_{n-1})(U_n - U_{n-1}) - \mathcal{F}(\mathbf{x}, U^*, \nabla U^*)] \cdot [\Delta \varphi - S \varphi + D\mathcal{F}(\mathbf{x}, U_{n-1}, \nabla U_{n-1})(\varphi)] d\mathbf{x} + \epsilon \langle U_n, \varphi \rangle_{H^2(\Omega)^N} = 0. \quad (5.12)$$

Let $\varphi_i = U_i - U^* - \mathcal{E} \in H_0$ for all $i \geq 1$ where \mathcal{E} is the vector in (5.2). Using the test function $\varphi = \varphi_n$ in (5.12) gives

$$\int_{\Omega} e^{2\lambda b^{-\beta} r^{\beta}(\mathbf{x})} [\Delta(\varphi_n + \mathcal{E}) - S(\varphi_n + \mathcal{E}) + D\mathcal{F}(\mathbf{x}, U_{n-1}, \nabla U_{n-1})(\varphi_n) + \mathcal{F}(\mathbf{x}, U_{n-1}, \nabla U_{n-1}) - \mathcal{F}(\mathbf{x}, U^*, \nabla U^*) - D\mathcal{F}(\mathbf{x}, U_{n-1}, \nabla U_{n-1})(\varphi_{n-1})] \cdot [\Delta \varphi_n - S \varphi_n + D\mathcal{F}(\mathbf{x}, U_{n-1}, \nabla U_{n-1})(\varphi_n)] d\mathbf{x} + \epsilon \langle \varphi_n + \mathcal{E} + U^*, \varphi_n \rangle_{H^2(\Omega)^N} = 0. \quad (5.13)$$

It follows from (5.13) that

$$\int_{\Omega} e^{2\lambda b^{-\beta} r^{\beta}(\mathbf{x})} \left| \Delta \varphi_n - S \varphi_n + D\mathcal{F}(\mathbf{x}, U_{n-1}, \nabla U_{n-1})(\varphi_n) \right|^2 d\mathbf{x} + \epsilon \|\varphi_n\|_{H^2(\Omega)^N}^2 + \epsilon \langle \mathcal{E}, \varphi_n \rangle_{H^2(\Omega)^N} + \epsilon \langle U^*, \varphi_n \rangle_{H^2(\Omega)^N} = \int_{\Omega} e^{2\lambda b^{-\beta} r^{\beta}(\mathbf{x})} [\mathcal{F}(\mathbf{x}, U^*, \nabla U^*) - \mathcal{F}(\mathbf{x}, U_{n-1}, \nabla U_{n-1}) + D\mathcal{F}(\mathbf{x}, U_{n-1}, \nabla U_{n-1})(\varphi_{n-1})] \cdot [\Delta \varphi_n - S \varphi_n + D\mathcal{F}(\mathbf{x}, U_{n-1}, \nabla U_{n-1})(\varphi_n)] d\mathbf{x} + \int_{\Omega} e^{2\lambda b^{-\beta} r^{\beta}(\mathbf{x})} [\Delta \mathcal{E} - S \mathcal{E}] \cdot [\Delta \varphi_n - S \varphi_n + D\mathcal{F}(\mathbf{x}, U_{n-1}, \nabla U_{n-1})(\varphi_n)] d\mathbf{x}. \quad (5.14)$$

Using the inequality $|ab| \leq a^2 + \frac{1}{4}b^2$ and (5.14), we have

$$\begin{aligned} & \int_{\Omega} e^{2\lambda b^{-\beta} r^{\beta}(\mathbf{x})} \left| \Delta \varphi_n - S\varphi_n + D\mathcal{F}(\mathbf{x}, U_{n-1}, \nabla U_{n-1})(\varphi_n) \right|^2 d\mathbf{x} + \epsilon \|\varphi_n\|_{H^2(\Omega)^N}^2 + \epsilon \langle \mathcal{E}, \varphi_n \rangle_{H^2(\Omega)^N} \\ & + \epsilon \langle U^*, \varphi_n \rangle_{H^2(\Omega)^N} \leq C \int_{\Omega} e^{2\lambda b^{-\beta} r^{\beta}(\mathbf{x})} \left| \mathcal{F}(\mathbf{x}, U^*, \nabla U^*) - \mathcal{F}(\mathbf{x}, U_{n-1}, \nabla U_{n-1}) \right. \\ & \quad \left. + D\mathcal{F}(\mathbf{x}, U_{n-1}, \nabla U_{n-1})(\varphi_{n-1}) \right|^2 d\mathbf{x} + C \int_{\Omega} e^{2\lambda b^{-\beta} r^{\beta}(\mathbf{x})} |\Delta \mathcal{E} - S\mathcal{E}|^2 d\mathbf{x}. \end{aligned} \quad (5.15)$$

Recall the inequality $(a - b)^2 \geq \frac{1}{2}a^2 - b^2$. We have

$$\begin{aligned} & \int_{\Omega} e^{\lambda b^{-\beta} r^{\beta}(\mathbf{x})} \left| \Delta \varphi_n - S\varphi_n + D\mathcal{F}(\mathbf{x}, U_{n-1}, \nabla U_{n-1})(\varphi_n) \right|^2 d\mathbf{x} \\ & \geq \frac{1}{2} \int_{\Omega} e^{\lambda b^{-\beta} r^{\beta}(\mathbf{x})} \left| \Delta \varphi_n \right|^2 d\mathbf{x} - \int_{\Omega} e^{\lambda b^{-\beta} r^{\beta}(\mathbf{x})} \left| -S\varphi_n + D\mathcal{F}(\mathbf{x}, U_{n-1}, \nabla U_{n-1})(\varphi_n) \right|^2 d\mathbf{x}. \end{aligned} \quad (5.16)$$

On the other hand, since $\|\mathcal{F}\|_{C^2} < \infty$, we can find a constant C such that

$$\begin{aligned} & \left| \mathcal{F}(\mathbf{x}, U^*, \nabla U^*) - \mathcal{F}(\mathbf{x}, U_{n-1}, \nabla U_{n-1}) + D\mathcal{F}(\mathbf{x}, U_{n-1}, \nabla U_{n-1})(\varphi_{n-1}) \right| \\ & \leq C(|\varphi_{n-1}| + |\nabla \varphi_{n-1}|), \end{aligned} \quad (5.17)$$

and

$$\left| -S\varphi_n + D\mathcal{F}(\mathbf{x}, U_{n-1}, \nabla U_{n-1})(\varphi_n) \right| \leq C(|\varphi_n| + |\nabla \varphi_n|) \quad (5.18)$$

for all $\mathbf{x} \in \bar{\Omega}$. Combining (5.15), (5.16), (5.17), (5.18) and the inequality $|ab| \leq \frac{1}{2}a^2 + \frac{1}{2}b^2$ gives

$$\begin{aligned} & \int_{\Omega} e^{2\lambda b^{-\beta} r^{\beta}(\mathbf{x})} \left| \Delta \varphi_n \right|^2 d\mathbf{x} + \epsilon \|\varphi_n\|_{H^2(\Omega)^N}^2 \leq C \int_{\Omega} e^{\lambda b^{-\beta} r^{\beta}(\mathbf{x})} (|\varphi_n|^2 + |\nabla \varphi_n|^2 + |\varphi_{n-1}|^2 \\ & + |\nabla \varphi_{n-1}|^2) d\mathbf{x} + C \int_{\Omega} e^{2\lambda b^{-\beta} r^{\beta}(\mathbf{x})} |\Delta \mathcal{E} - S\mathcal{E}|^2 d\mathbf{x} + C\epsilon \|U\|_{H^2(\Omega)^2}^2 + C\epsilon \|\mathcal{E}\|_{H^2(\Omega)^2}^2 + C\epsilon \|\varphi_n\|_{H^2(\Omega)^N}^2, \end{aligned}$$

which implies

$$\begin{aligned} & \int_{\Omega} e^{\lambda b^{-\beta} r^{\beta}(\mathbf{x})} \left| \Delta \varphi_n \right|^2 d\mathbf{x} \leq C \int_{\Omega} e^{\lambda b^{-\beta} r^{\beta}(\mathbf{x})} (|\varphi_n|^2 + |\nabla \varphi_n|^2 + |\varphi_{n-1}|^2 + |\nabla \varphi_{n-1}|^2) d\mathbf{x} \\ & \quad + C \int_{\Omega} e^{2\lambda b^{-\beta} r^{\beta}(\mathbf{x})} |\Delta \mathcal{E} - S\mathcal{E}|^2 d\mathbf{x} + C\epsilon \|\mathcal{E}\|_{H^2(\Omega)^2}^2 + C\epsilon \|U^*\|_{H^2(\Omega)^2}^2. \end{aligned} \quad (5.19)$$

We now apply the Carleman estimate in Corollary 4.1. Using (4.10) for each component of the vector φ_n , we have

$$\begin{aligned} & \int_{\Omega} e^{2\lambda b^{-\beta} r^{\beta}(\mathbf{x})} |\Delta \varphi_n|^2 d\mathbf{x} \geq C\lambda^{-1} \int_{\Omega} e^{2\lambda b^{-\beta} r^{\beta}(\mathbf{x})} |D^2 \varphi_n|^2 d\mathbf{x} \\ & \quad + C\lambda^3 \int_{\Omega} e^{2\lambda b^{-\beta} r^{\beta}(\mathbf{x})} |\varphi_n|^2 d\mathbf{x} + C\lambda \int_{\Omega} e^{2\lambda b^{-\beta} r^{\beta}(\mathbf{x})} |\nabla \varphi_n|^2 d\mathbf{x} \end{aligned} \quad (5.20)$$

Using (5.19) and (5.20), we have

$$\begin{aligned}
& \lambda^{-1} \int_{\Omega} e^{2\lambda b^{-\beta} r^{\beta}(\mathbf{x})} |D^2 \varphi_n|^2 d\mathbf{x} + \lambda^3 \int_{\Omega} e^{2\lambda b^{-\beta} r^{\beta}} |\varphi_n|^2 d\mathbf{x} + \lambda \int_{\Omega} e^{2\lambda b^{-\beta} r^{\beta}(\mathbf{x})} |\nabla \varphi_n|^2 d\mathbf{x} \\
& \leq C \int_{\Omega} e^{\lambda b^{-\beta} r^{\beta}(\mathbf{x})} (|\varphi_n|^2 + |\nabla \varphi_n|^2 + |\varphi_{n-1}|^2 + |\nabla \varphi_{n-1}|^2) d\mathbf{x} \\
& \quad + C \int_{\Omega} e^{2\lambda b^{-\beta} r^{\beta}(\mathbf{x})} |\Delta \mathcal{E} - S\mathcal{E}|^2 d\mathbf{x} + C\epsilon \|\mathcal{E}\|_{H^2(\Omega)}^2 + C\epsilon \|U^*\|_{H^2(\Omega)}^2. \quad (5.21)
\end{aligned}$$

Since λ is large, we can write (5.21) as

$$\begin{aligned}
& \lambda^{-1} \int_{\Omega} e^{2\lambda b^{-\beta} r^{\beta}(\mathbf{x})} |D^2 \varphi_n|^2 d\mathbf{x} + \lambda^3 \int_{\Omega} e^{2\lambda b^{-\beta} r^{\beta}} |\varphi_n|^2 d\mathbf{x} + \lambda \int_{\Omega} e^{2\lambda b^{-\beta} r^{\beta}(\mathbf{x})} |\nabla \varphi_n|^2 d\mathbf{x} \\
& \leq C \int_{\Omega} e^{\lambda b^{-\beta} r^{\beta}(\mathbf{x})} (|\varphi_{n-1}|^2 + |\nabla \varphi_{n-1}|^2) d\mathbf{x} + C \int_{\Omega} e^{2\lambda b^{-\beta} r^{\beta}(\mathbf{x})} |\Delta \mathcal{E} - S\mathcal{E}|^2 d\mathbf{x} \\
& \quad + C\epsilon \|\mathcal{E}\|_{H^2(\Omega)}^2 + C\epsilon \|U^*\|_{H^2(\Omega)}^2. \quad (5.22)
\end{aligned}$$

It follows from (5.22) that

$$\begin{aligned}
& \int_{\Omega} e^{2\lambda b^{-\beta} r^{\beta}(\mathbf{x})} (\lambda^{-2} |D^2 \varphi_n|^2 + |\varphi_n|^2 + |\nabla \varphi_n|^2) d\mathbf{x} \\
& \leq \frac{C}{\lambda} \int_{\Omega} e^{\lambda b^{-\beta} r^{\beta}(\mathbf{x})} (|\varphi_{n-1}|^2 + |\nabla \varphi_{n-1}|^2) d\mathbf{x} + \frac{1}{2\lambda} \epsilon \|U\|_{H^2(\Omega)}^2 \\
& \leq \frac{C}{\lambda} \int_{\Omega} e^{\lambda b^{-\beta} r^{\beta}(\mathbf{x})} (\lambda^{-2} |D^2 \varphi_{n-1}|^2 + |\varphi_{n-1}|^2 + |\nabla \varphi_{n-1}|^2) d\mathbf{x} \\
& \quad + \frac{C}{\lambda} \left[\int_{\Omega} e^{2\lambda b^{-\beta} r^{\beta}(\mathbf{x})} |\Delta \mathcal{E} - S\mathcal{E}|^2 d\mathbf{x} + \epsilon \|\mathcal{E}\|_{H^2(\Omega)}^2 + \epsilon \|U^*\|_{H^2(\Omega)}^2 \right]. \quad (5.23)
\end{aligned}$$

It follows from (5.23) and by induction, we have

$$\begin{aligned}
& \int_{\Omega} e^{2\lambda b^{-\beta} r^{\beta}(\mathbf{x})} (\lambda^{-2} |D^2 \varphi_n|^2 + |\varphi_n|^2 + |\nabla \varphi_n|^2) d\mathbf{x} \\
& \leq \left(\frac{C}{\lambda}\right)^{n+1} \int_{\Omega} e^{\lambda b^{-\beta} r^{\beta}(\mathbf{x})} (\lambda^{-2} |D^2 \varphi_0|^2 + |\varphi_0|^2 + |\nabla \varphi_0|^2) d\mathbf{x} \\
& \quad + \frac{C/\lambda}{1 - C/\lambda} \left[\int_{\Omega} e^{2\lambda b^{-\beta} r^{\beta}(\mathbf{x})} |\Delta \mathcal{E} - S\mathcal{E}|^2 d\mathbf{x} + \epsilon \|\mathcal{E}\|_{H^2(\Omega)}^2 + \epsilon \|U^*\|_{H^2(\Omega)}^2 \right] \quad (5.24)
\end{aligned}$$

Recall $\varphi_i = U_i - U^* - \mathcal{E}$, $i \geq 0$. Using (5.24) and inequalities $(a - b)^2 \geq \frac{1}{2}a^2 - b^2$ and $(a + b)^2 \leq 2a^2 + 2b^2$, we obtain (5.5). \square

Theorem 5.1 and Corollary 5.2 suggest Algorithm 2 to solve the inverse source problem under consideration.

Remark 5.4 (The case when $\|\mathcal{F}\|_{C^2} = \infty$). *The condition $\|\mathcal{F}\|_{C^2} < \infty$ in Theorem 5.1 is too strong. It can be relaxed in the context when the forward problem has a unique and bounded solution as in Assumption 1.1. Assume that $p^* \in \mathcal{P}$, see Definition 1.1 for the definition of \mathcal{P} . Then, we can apply the truncation technique as in the proof of Theorem 2.1 to compute U^* . Since solution of*

Algorithm 2 The procedure to compute the numerical solution to Problem 1.1

- 1: Choose a basis $\{\Psi_n\}_{n \geq 1}$ of $L^2(0, T)$. Choose a cut-off number $N > 0$. See Section 6.1 and Figure 1 for a reasonable choice of N .
 - 2: Compute the vector valued functions G_0 and G_1 as in (3.11) and (3.12).
 - 3: Apply Algorithm 1 to compute a numerical solution U^{comp} to (3.13).
 - 4: Reconstruct the source function by the first formula in (5.7).
-

the forward problem is bounded as in Assumption 1.1, it follows from (3.2) that the true solution U^* to (5.4) is bounded, namely,

$$|U^*| + |\nabla U^*| < B$$

for some number B . Define χ_B as in (2.3) and $\mathcal{F}_B = \chi_B \mathcal{F}$. Clearly, the vector valued function U^* satisfies

$$\begin{cases} \Delta U^* - S U^* + \mathcal{F}_B(\mathbf{x}, U^*, \nabla U^*) = 0 & \mathbf{x} \in \Omega, \\ U^*(\mathbf{x}) = G_0^*(\mathbf{x}) & \mathbf{x} \in \partial\Omega, \\ \partial_\nu U^*(\mathbf{x}) = G_1^*(\mathbf{x}) & \mathbf{x} \in \partial\Omega \end{cases} \quad (5.25)$$

Since \mathcal{F}_B has a bounded C^2 norm, we can apply Algorithm 1 for (5.25) to compute U^* .

6 Numerical Simulations

In this section, we will illustrate the theoretical results by some numerical examples. For simplicity, we implement Algorithms 1 and 2 in 2D and in the finite difference scheme. The set Ω is the square $(-R, R)^2$ where $R = 1$. We solve the forward problem on a larger domain $\Omega_1 := (-R_1, R_1)^2$ where $R_1 = 6$. We will use the notation $\mathbf{x} = (x, y)$ to represent points on Ω . We arrange a uniform $N_x^1 \times N_x^1$ grid, named as \mathcal{G} , on Ω_1 as follows

$$\mathcal{G}_1 = \{(x_i, y_j) : x_i = -R_1 + (i-1)h_x, y_j = -R_1 + (j-1)h_x, i, j = 1, \dots, N_x^1\}$$

where $N_x^1 = 240$ and $h_x = 2R_1/(N_x^1 - 1)$. We also choose $T = 1.5$ and divide the interval $[0, T]$ uniformly into $N_t = 3000$ uniform subintervals. For the forward data generation, we solve (1.1) by the explicit method. We then collect the (noiseless) data $g_0(\mathbf{x}, t) = u(\mathbf{x}, t)$ and $g_1(\mathbf{x}, t) = \partial_\nu u(\mathbf{x}, t)$ on the lateral boundary $\partial\Omega_T$. Noise is then added to the data using the following expression:

$$g_i^\delta(x, t) = g_i(x, t)[1 + \delta(-1 + 2\eta(x, t))], i = 0, 1 \quad (6.1)$$

where δ denotes the noise level and $\eta(x, t)$ generates uniformly distributed numbers in the interval $[-1, 1]$. The implementation of Algorithm 2 to reconstruct the source function from the noisy data is given in the next subsection. We would also like to remark here that the inversion algorithm has been implemented on the uniform grid $\mathcal{G} = \mathcal{G}_1 \cap \bar{\Omega}$.

6.1 Implementation

We now describe the steps to implement Algorithm 2 which enable us to reconstruct the source function in this inverse source problem.

Step 1: Following the arguments laid out in Section 3, (also see [23, Section 5.2]), in Step 1 of Algorithm 2, we choose the special basis functions $\{\Psi_n\}_{n \geq 1}$ of the space $L^2(0, T)$, which was

originally introduced by Klivanov in [16]. We recall that Klivanov's basis is obtained by applying the Gram-Schmidt orthogonalization process for the sequence of functions $\{\Phi_n(t)\}_{n \geq 1}$ where $\Phi_n(t) = t^{n-1}e^{t-T/2}$. A comparative advantage of this special basis over traditional trigonometric Fourier basis is that the first term of the trigonometric basis being a constant, vanishes on taking the derivatives. As such, there will be no contribution from the coefficient of the first basis function on the left hand side of equation (3.4), i.e. the information from $u_1(x)\Psi_1'(t)$ is lost, while this information is retained if we use Klivanov's basis. To choose the cut off number N , we take the data $u(\mathbf{x}, t)$ for $\mathbf{x} \in \Gamma$ and $t \in (0, T)$ where

$$\Gamma = \{\mathbf{x} = (x, y = R) : |x| \leq R\} \subset \partial\Omega.$$

We then compute the function

$$e_N(\mathbf{x}, t) = |u(\mathbf{x}, t) - \sum_{n=1}^N u_n(\mathbf{x})\Psi_n(t)|$$

where u_n is as in (3.2). This step of choosing N by evaluating e_N for different values of N is illustrated in Figure 1. Here, u solves equation (1.1) with p given as in test 2 below.

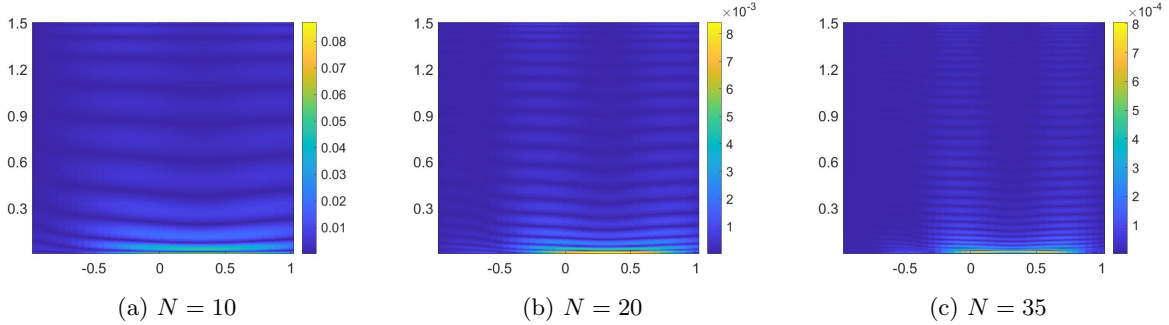


Figure 1: The graphs of the functions $e_N(\mathbf{x}, t)$, $(\mathbf{x}, t) \in \Gamma \times (0, T)$. In the figure, the x-axis runs from -1 to 1 and the y-axis is from 0 to 1.5 . It is evident that when $N = 35$, the error function e_N is sufficiently small, say $\|e_N\|_{L^\infty} < 5 \times 10^{-2}$.

Step 2: Once the basis terms $\{\Psi_m\}_{m=1}^N$ are found out, one can easily evaluate the integrals given by equations 3.9 and 3.10. The computation of the (vector) data term as per equations (3.11) and (3.12) is straight forward.

Step 3: The implementation of Step 3 of Algorithm 2 or equivalently Algorithm 1 follows closely from that in [26]. In Step 1 of Algorithm 1, we need to choose the artificial parameters. The parameters for the Carleman weight function used in step 4 of Algorithm 1 are given by $r = |\mathbf{x} - \mathbf{x}_0|$ where $\mathbf{x}_0 = (0, 1.5)$, $b = 5$, $\lambda = 40$ and $\beta = 10$. The regularization parameter used was $\epsilon = 10^{-7}$. These values are chosen by a manual trial and error process. We use test 1 below as the reference test. We modify ϵ , λ , b , β , \mathbf{x}_0 until we obtain a satisfactory solution with noiseless data. These parameters are used for all other tests with all noise levels. In Step 2 of Algorithm 1, we compute the initial term of the sequence $\{U_n\}_{n \geq 0}$, i.e., U_0 . This function is found by solving the problem (3.13) wherein we use only the linear part of the term $\mathcal{F}(x, U, \nabla U)$ denoted by $\mathcal{F}_{lin}(U)$. The (vector) term $\mathcal{F}_{lin}(U)$ is computed from (3.7) by evaluating for each m in the following way: Suppose the term $F(x, u, \nabla u)$ appearing in the integral in (3.7) is given by $F(x, u, \nabla u) = F_{lin}(u) + \text{non-linear terms}$. For example,

for the first test given in the next subsection, $F(x, u, \nabla u) = u(1 - u) = \underbrace{u}_{\text{linear part}} - \underbrace{u^2}_{\text{non-linear part}}$.

Similarly, for the second test, $F(x, u, \nabla u) = \underbrace{u}_{\text{linearpart}} + \underbrace{\sqrt{(|\nabla u|^2 + 1)}}_{\text{non-linearpart}}$. Thus for both the tests, we

take $F_{lin}(u) = u$ which is then used in (3.7) in place of $F(x, u, \nabla u)$ to get $\mathcal{F}_{lin}(U)$. Now to generate the initial guess we solve the following system:

$$\begin{cases} \Delta U - SU + \mathcal{F}_{lin}(U) = 0 & \mathbf{x} \in \Omega, \\ U(\mathbf{x}) = G_0(\mathbf{x}) & \mathbf{x} \in \partial\Omega, \\ \partial_\nu U(\mathbf{x}) = G_1(\mathbf{x}) & \mathbf{x} \in \partial\Omega. \end{cases} \quad (6.2)$$

Next, the minimizer of the corresponding (strictly) convex linear functional $J_n(\phi)$ appearing in Step 4 of algorithm 1 can be found by solving the corresponding Normal equation. For brevity, we do not describe the finite difference implementation of various operators appearing in the expression for the Normal equation corresponding to $J_n(\phi)$ as these are similar to those discussed elsewhere, see e.g. [23, section 5.3]. We briefly mention that the matrix forms of all such operators is necessarily stored as sparse matrices. Solution to this Normal equation is then found by using the MATLAB function 'lsqlin' which in turn is the minimizer of the functional $J_n(\phi)$ on H_0 . We let the iterative Algorithm 1 run for six iterations, i.e. $n = 6$ as it was observed that $\|U_6 - U_5\|_{L^\infty}$ was small enough in all numerical experiments.

Step 4: From the computed solution $U^{comp} = U_6$, one can reconstruct the source function as described in Step 4 of Algorithm 2.

6.2 Numerical examples

Test 1. The true source function is given by:

$$p_{true} = \begin{cases} 8, & \text{if } x^2 + (y - 0.3)^2 \leq 0.45^2 \\ 0, & \text{otherwise} \end{cases}$$

The nonlinearity considered in this case is given by:

$$F(x, u, \nabla u) = u(1 - u).$$

We notice that the position of the inclusion is correctly identified. Furthermore, the maximal computed value in the reconstruction at 20% noise level is 6.89 for a relative error of 13.87% in the reconstruction.

Test 2. The true source function is given by:

$$p_{true} = \begin{cases} 12, & \text{if } (x - 0.5)^2 + (y - 0.5)^2 \leq 0.35^2 \\ 10, & \text{if } (x + 0.5)^2 + (y + 0.5)^2 \leq 0.35^2 \\ 14, & \text{if } (x - 0.5)^2 + (y + 0.5)^2 \leq 0.35^2 \\ 9, & \text{if } (x - 0.5)^2 + (y - 0.5)^2 \leq 0.35^2 \\ 0, & \text{otherwise} \end{cases}$$

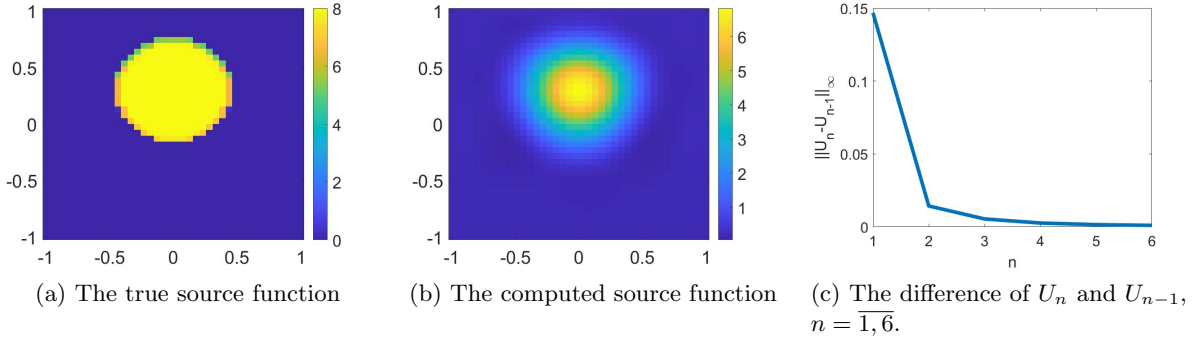


Figure 2: Test 1. (a) contains the true phantom p_{true} . (b) is the reconstruction of the phantom from noisy data after 6 iterations. (c) shows the convergence of the method by plotting $\|U_n - U_{n-1}\|_\infty$ against the number of iterations n . Noise level used in this experiment was 20%.

The nonlinearity considered in this case is given by:

$$F(x, u, \nabla u) = u + \sqrt{(|\nabla u|^2 + 1)}.$$

Again, we notice, that the positions of all four inclusions are correctly identified. The maximal

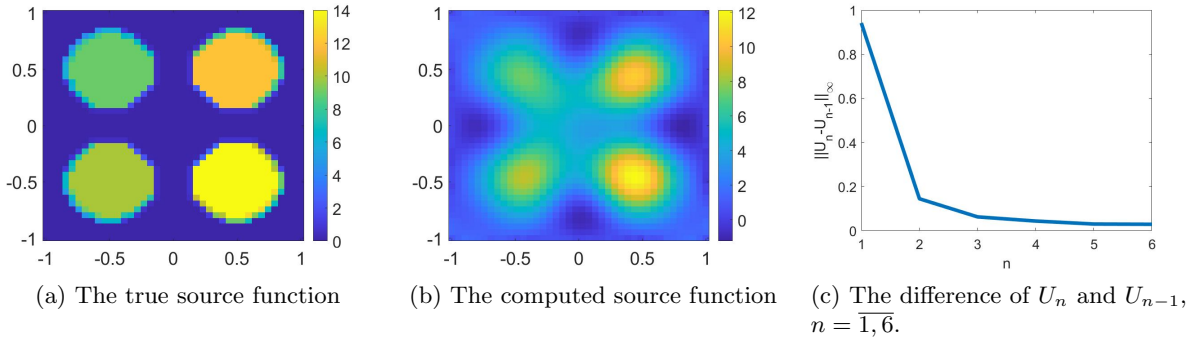


Figure 3: Test 2. (a) contains the true phantom p_{true} . (b) is the reconstruction of the phantom from noisy data after 6 iterations. (c) shows the convergence of the method by plotting $\|U_n - U_{n-1}\|_\infty$ against the number of iterations n . Noise level used in this experiment was 20%.

computed values in the reconstructions of the four inclusions at 20% noise level are 10.66 (up, right), 12.01 (down, right), 7.33 (up, left) and 8.60 (down, left), for relative errors of 11.16%, 13.57%, 8.37% and 14% respectively.

Remark 6.1. *In our numerical experiments, we tried several noise levels from 1% to 20% with the quality of reconstruction not deteriorating by any appreciable amount at higher levels of noise. We have provided the reconstructions at 20% noise level here. This shows a very high degree of the robustness of our reconstructions compared to the noise-level. This fact is also borne out by figure 4 in which we have compared the quality of reconstruction across the pixels lying on the vertical line passing through $x = 0.5$ for the phantom in Test 2.*

We recall two main facts to interpret the strong stability of our method with respect to noise, see (6.1). The first one is that we have truncated all high frequency components of the data while the lower frequency components are not sensitive with the noise. The second fact is that we have reduced the inverse problem to the problem of solving elliptic equations given boundary data, which is known to be stable. The stability is guaranteed by Theorem 5.1, Corollary 5.1 and the estimate (5.6).

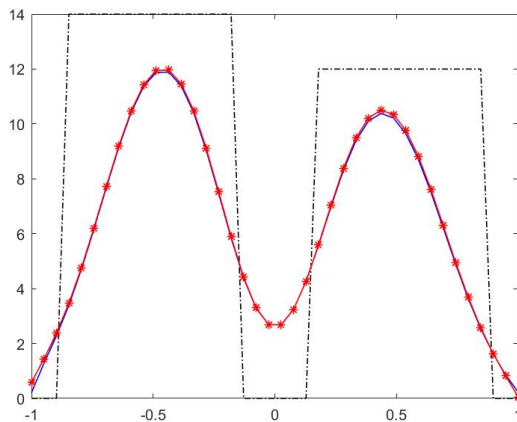


Figure 4: The true phantom (dashed, black), reconstruction at 5% noise level (red, -*) and reconstruction at 20% noise level (solid, blue) on the vertical line passing through $x = 0.5$ in phantom for test 2. The horizontal axis in the plot refers to the y-axis of the phantom and the vertical axis gives the pixel values. Reconstruction at 20% noise level is only very slightly worse than that at 5% noise level.

It is remarkable that in the tests above, the value of the source inside the inclusions are high. Hence, the locally convergent approaches based on optimization, which require a good initial guess of the true solution, might not be applicable. Unlike this, our methods provide reliable solutions.

7 Concluding remarks

In this paper, we introduce an iterative method to solve an inverse source problem for a nonlinear parabolic equations. This method can be considered as the combination of Carleman estimates and the Newton method in solving nonlinear equations. In the first step, we truncate the Fourier series of the solution to the governing equation to derive a system of nonlinear elliptic equations. The computed solution to this system yields directly the solution for the inverse source problem. In order to compute such a solution, we repeatedly solve the linearization of this system. By using Carleman estimate, we proved that the sequence of obtained solutions to the desired solution. The strength of our numerical method is that it quickly provides a good approximation to the true source function. Furthermore, it does not require any knowledge of the true source function. This means a good initial guess is not necessary.

The method was implemented in finite difference. Numerical results were shown.

Acknowledgement

The works of TTL and LHN were partially supported by National Science Foundation grant DMS-2208159, and by funds provided by the Faculty Research Grant program at UNC Charlotte Fund No. 111272.

References

- [1] A. B. Bakushinskii, M. V. Klibanov, and N. A. Koshev. Carleman weight functions for a globally convergent numerical method for ill-posed Cauchy problems for some quasilinear PDEs. *Nonlinear Anal. Real World Appl.*, 34:201–224, 2017.
- [2] L. Baudouin, M. de Buhan, and S. Ervedoza. Convergent algorithm based on Carleman estimates for the recovery of a potential in the wave equation. *SIAM J. Numer. Anal.*, 55:1578–1613, 2017.
- [3] L. Borcea, V. Druskin, A. V. Mamonov, and M. Zaslavsky. A model reduction approach to numerical inversion for a parabolic partial differential equation. *Inverse Problems*, 30:125011, 2014.
- [4] M Boulakia, M. de Buhan, and E. Schwindt. Numerical reconstruction based on Carleman estimates of a source term in a reaction-diffusion equation. *ESAIM: COCV*, 2021.
- [5] K. Cao and D. Lesnic. Determination of space-dependent coefficients from temperature measurements using the conjugate gradient method. *Numer Methods Partial Differential Eq.*, 34:1370–1400, 2018.
- [6] K. Cao and D. Lesnic. Simultaneous reconstruction of the perfusion coefficient and initial temperature from time-average integral temperature measurements. *Applied Mathematical Modelling*, 68:523–539, 2019.
- [7] A. El Badia and T. Ha-Duong. On an inverse source problem for the heat equation. application to a pollution detection problem. *Journal of Inverse and Ill-posed Problems*, 10:585–599, 2002.
- [8] R. A. Fisher. The wave of advance of advantageous genes. *Annals of Eugenics*, 7(4):355–369, 1937.
- [9] M. Haltmeier and L. V. Nguyen. Analysis of iterative methods in photoacoustic tomography with variable sound speed. *SIAM J. Imaging Sci.*, 10:751–781, 2017.
- [10] V. Katsnelson and L. V. Nguyen. On the convergence of time reversal method for thermoacoustic tomography in elastic media. *Applied Mathematics Letters*, 77:79–86, 2018.
- [11] Y. L. Keung and J. Zou. Numerical identifications of parameters in parabolic systems. *Inverse Problems*, 14:83–100, 1998.
- [12] V. A. Khoa, G. W. Bidney, M. V. Klibanov, L. H. Nguyen, L. Nguyen, A. Sullivan, and V. N. Astratov. Convexification and experimental data for a 3D inverse scattering problem with the moving point source. *Inverse Problems*, 36:085007, 2020.

- [13] V. A. Khoa, G. W. Bidney, M. V. Klibanov, L. H. Nguyen, L. Nguyen, A. Sullivan, and V. N. Astratov. An inverse problem of a simultaneous reconstruction of the dielectric constant and conductivity from experimental backscattering data. *Inverse Problems in Science and Engineering*, 29(5):712–735, 2021.
- [14] V. A. Khoa, M. V. Klibanov, and L. H. Nguyen. Convexification for a 3D inverse scattering problem with the moving point source. *SIAM J. Imaging Sci.*, 13(2):871–904, 2020.
- [15] M. V. Klibanov. Estimates of initial conditions of parabolic equations and inequalities via lateral Cauchy data. *Inverse Problems*, 22:495–514, 2006.
- [16] M. V. Klibanov. Convexification of restricted Dirichlet to Neumann map. *J. Inverse and Ill-Posed Problems*, 25(5):669–685, 2017.
- [17] M. V. Klibanov and O. V. Ioussoupova. Uniform strict convexity of a cost functional for three-dimensional inverse scattering problem. *SIAM J. Math. Anal.*, 26:147–179, 1995.
- [18] M. V. Klibanov, L. H. Nguyen, and H. V. Tran. Numerical viscosity solutions to Hamilton-Jacobi equations via a Carleman estimate and the convexification method. *Journal of Computational Physics*, 451:110828, 2022.
- [19] O. A. Ladyzhenskaya, V.A. Solonnikov, and N. N. Ural'tseva. *Linear and quasilinear equations of Parabolic Type*, volume 23. American Mathematical Society, Providence, RI, 1968.
- [20] R. Lattès and J. L. Lions. *The Method of Quasireversibility: Applications to Partial Differential Equations*. Elsevier, New York, 1969.
- [21] M. M. Lavrent'ev, V. G. Romanov, and S. P. Shishat'skii. *Ill-Posed Problems of Mathematical Physics and Analysis*. Translations of Mathematical Monographs. AMS, Providence: RI, 1986.
- [22] T. T. Le. Global reconstruction of initial conditions of nonlinear parabolic equations via the Carleman-contraction method. *preprint, arXiv:2205.10648*, 2022.
- [23] T. T. Le and L. H. Nguyen. A convergent numerical method to recover the initial condition of nonlinear parabolic equations from lateral Cauchy data. *Journal of Inverse and Ill-posed Problems*, 30(2):265–286, 2022.
- [24] T. T. Le and L. H. Nguyen. The gradient descent method for the convexification to solve boundary value problems of quasi-linear PDEs and a coefficient inverse problem. *Journal of Scientific Computing*, 91(3):74, 2022.
- [25] T. T. Le, L. H. Nguyen, T-P. Nguyen, and W. Powell. The quasi-reversibility method to numerically solve an inverse source problem for hyperbolic equations. *Journal of Scientific Computing*, 87:90, 2021.
- [26] T. T. Le, L. H. Nguyen, and H. V. Tran. A Carleman-based numerical method for quasilinear elliptic equations with over-determined boundary data and applications. *Computers and Mathematics with Applications*, 125(2022), 13-24.
- [27] J. Li, H. Liu, and H. Sun. On a gesture-computing technique using electromagnetic waves. *Inverse Probl. Imaging*, 12:677–696, 2018.

- [28] J. Li, M. Yamamoto, and J. Zou. Conditional stability and numerical reconstruction of initial temperature. *Communications on Pure and Applied Analysis*, 8:361–382, 2009.
- [29] Q. Li and L. H. Nguyen. Recovering the initial condition of parabolic equations from lateral Cauchy data via the quasi-reversibility method. *Inverse Problems in Science and Engineering*, 28:580–598, 2020.
- [30] H. Liu and G. Uhlmann. Determining both sound speed and internal source in thermo- and photo-acoustic tomography. *Inverse Problems*, 31:105005, 2015.
- [31] D-L Nguyen, L. H. Nguyen, and T. Truong. The Carleman-based contraction principle to reconstruct the potential of nonlinear hyperbolic equations. *preprint, arXiv:2204.06060*, 2022.
- [32] L. H. Nguyen. A new algorithm to determine the creation or depletion term of parabolic equations from boundary measurements. *Computers and Mathematics with Applications*, 80:2135–2149, 2020.
- [33] L. H. Nguyen. The Carleman-contraction method to solve quasi-linear elliptic equations. *preprint, 2022*.
- [34] L. H. Nguyen and M. V. Klibanov. Carleman estimates and the contraction principle for an inverse source problem for nonlinear hyperbolic equations. *Inverse Problems*, 38:035009, 2022.
- [35] L. H. Nguyen, Q. Li, and M. V. Klibanov. A convergent numerical method for a multi-frequency inverse source problem in inhomogenous media. *Inverse Problems and Imaging*, 13:1067–1094, 2019.
- [36] P. M. Nguyen and L. H. Nguyen. A numerical method for an inverse source problem for parabolic equations and its application to a coefficient inverse problem. *Journal of Inverse and Ill-posed Problems*, 38:232–339, 2020.
- [37] X. Wang, Y. Guo, J. Li, and H. Liu. Mathematical design of a novel input/instruction device using a moving acoustic emitter. *Inverse Problems*, 33:105009, 2017.
- [38] X. Wang, Y. Guo, D. Zhang, and H. Liu. Fourier method for recovering acoustic sources from multi-frequency far-field data. *Inverse Problems*, 33:035001, 2017.
- [39] L. Yang, J-N. Yu, and Y-C. Deng. An inverse problem of identifying the coefficient of parabolic equation. *Applied Mathematical Modelling*, 32:1984–1995, 2008.
- [40] D. Zhang, Y. Guo, J. Li, and H. Liu. Retrieval of acoustic sources from multi-frequency phaseless data. *Inverse Problems*, 34:094001, 2018.